Expression profiles of long noncoding RNAs and mRNAs in post-cardiac arrest rat brains

RONG LIU[1], XIAOXING LIAO[2], XIN LI[3], HONGYAN WEI[2], QING LIANG[1], ZUOPENG ZHANG[1], MEIXIAN YIN[2], XIAOYUN ZENG[2], ZIJING LIANG[1] and CHUNLIN HU[2]

[1]Department of Emergency, The First Affiliated Hospital, Guangzhou Medical University, Guangzhou, Guangdong 510120; [2]Department of Emergency, The First Affiliated Hospital, Sun Yat-sen University; [3]Department of Emergency, Guangdong Provincial People's Hospital, Guangzhou, Guangdong 510080, P.R. China

Received September 1, 2017; Accepted March 1, 2018

DOI: 10.3892/mmr.2018.8703

Abstract. To investigate long noncoding (lnc)-RNA and mRNA expression profiles in post-cardiac arrest (CA) brains, an external transthoracic electrical current was applied for 8 min to induce CA (the CA group). A total of 4 rats received sham-operations and served as the blank control (BC) group. Upon return of spontaneous circulation (ROSC), lncRNA and mRNA expression in the rat cerebral cortex was assayed with high-throughput Agilent lncRNA and mRNA microarrays. In total, 37 lncRNAs were upregulated and 21 lncRNAs were downregulated in the CA group, and 258 mRNA transcripts were differentially expressed with 177 mRNAs upregulated and 81 mRNAs downregulated in the CA group. The differentially expressed lncRNAs in the CA group were co-expressed with thousands of mRNAs. The differentially expressed lncRNAs could be clustered into >100 signaling pathways and processes according to Gene Ontology, and Kyoto Encyclopedia of Genes and Genomes analyses. The most common predicted functions involved metabolic pathways, protein synthesis, transport and degradation during CA-ROSC. CA-ROSC led to significant alterations in cerebral lncRNA and mRNA expression profiles. Thus, lncRNA-mRNA network interactions have the potential to regulate vital metabolic pathways and processes involved in CA-ROSC.

Correspondence to: Dr Chunlin Hu, Department of Emergency, The First Affiliated Hospital, Sun Yat-sen University, 58 Zhongshan Road II, Guangzhou, Guangdong 510080, P.R. China
E-mail: hu-chunlin@163.com

Dr Zijing Liang, Department of Emergency, The First Affiliated Hospital, Guangzhou Medical University, 151 Yanjiang Road, Guangzhou, Guangdong 510120, P.R. China
E-mail: 13719337897@163.com

Key words: long non-coding RNA, post-cardiac arrest, cerebral damage, microarray, signal pathway

Introduction

Cardiac arrest (CA) is a very dangerous state of shock and is a common cause of mortality and disability because the whole body suffers from severe ischemia, including the cerebellum, thalamus, hippocampus, and cortex (1,2). Even if CA patients receive timely restoration of spontaneous circulation (ROSC), ischemia still may occur leading to an ischemia/reperfusion (I/R) injury, which includes apoptosis and necrosis of neurons and activation of multiple pathogenic mechanisms (1). The poor outcomes in CA patients due to these distinct pathologies is termed post-CA syndrome (2). The probability that CA patients will recover after ROSC is increasing because of increasing public knowledge of cardiopulmonary resuscitation (CPR), significant improvements in the construction of emergency networks, and rapid progress in rescue technology. Early diagnosis and proper evaluation of the severity of brain damage is necessary for good prognoses in CA patients. However, the exact etiology of I/R injury remains poorly understood in CA, and the cerebral pathology of I/R injury and the molecular mechanisms of I/R after CA-ROSC remains to be elucidated.

Thousands of messenger RNAs (mRNAs) are continuously transcribed and guide the translation of various proteins in the adult mammalian brain during pathological states. The transcriptional and translational machinery is comprised of a variety of molecules, such as DNA methylases, transcription factors, ribosomes, and RNA polymerases. Recently, noncoding RNAs have been shown to potently regulate gene expression at the levels of transcription and translation (3). These noncoding RNAs participate in cellular, developmental, and disease processes by regulating RNA and protein levels, imprinting, enhancer function, and transcription (4-7). Long noncoding RNAs (lncRNAs) are a relatively new class of RNA molecules that are longer than 200 nucleotides and much less well characterized than microRNAs. Cerebral lncRNA profiles have been shown to be markedly altered in many pathological states, to play important roles in the pathophysiology of central nervous system and brain-related diseases and disorders, and to have profound effects on disease outcomes (8-11). Notably, studies have also shown that lncRNAs are associated with I/R brain injury (11,12).

However, cerebral lncRNA profiles after CA-ROSC, including a complete list of lncRNAs expressed in the brain, have yet to be elucidated. In addition, the potential roles and effects of these lncRNAs on mRNA expression during the early stage of reperfusion have yet to be determined. Undoubtedly, understanding lncRNA and mRNA network profiles in post-CA brains could inform the development of therapeutics to prevent secondary neuronal death caused by CA. In this study, we used a rat model to explore lncRNA and mRNA network profiles in cortical pathophysiological processes to further understand the etiology and molecular mechanisms of cerebral pathology during an I/R injury.

Materials and methods

Animals. Male Wistar rats (15-16 months old and 305.5-400.3 g) were obtained from the Experimental Animal Center, Sun Yat-Sen University, Guangdong Province (Guangzhou, China). Animals were housed in a pathogen-free laboratory at 20-22˚C with a 10 h light and 14 h dark cycle. The animal studies were approved by the Institutional Animal Care and Use Committee of Sun Yat-sen University and the procedures used were in accordance with the Animal Research Reporting for *in vivo* Experiments Guidelines on animal research (13).

Induction of ventricular fibrillation (VF). After fasting overnight (with access to water), 14 healthy male Wistar rats were anesthetized by intraperitoneal pentobarbital injection (30 mg/kg; Sigma, Natick, MA, USA). VF was induced as described previously (14,15). VF was successfully induced by alternating current (50 Hz, 6 V) for 10 sec with external transthoracic needles. After successful induction of VF, the ventilator was disconnected. Eight min after VF, manual chest compressions were performed on the rats along with mechanical ventilation. Rats were maintained for 24 h after successful ROSC (CA, n=14). Seven sham-operated rats served as the blank control (BC, n=7). 5 rats in model group and 4 in sham group were anesthetized by intraperitoneal pentobarbital injection (40 mg/kg; Sigma), and were sacrificed by decapitation at ROSC 2 h, the cerebral cortex tissue were harvested for RNA analysis. The rest rats were survival to 24 h after ROSC and their neurological deficits scores (NDS) were assessed from 0 (no observed neurological deficit) to 500 (death or brain death) (14,15) by 2 investigators who were blinded to the treatment. All of the other animals were sacrificed at 24 h after ROSC; the brains were removed and were fixed using paraffin for Nissl and TdT-mediated dUTP-biotin nick end labeling (TUNEL) staining, the apoptotic cells were counted randomly 6 fields in sequence slice in each group. All rats were anesthetized by intraperitoneal pentobarbital injection (40 mg/kg) and were sacrificed by decapitation.

Tissue harvest and RNA extraction. The rat brains were harvested and the cerebral cortices were dissected quickly on ice. Samples of cerebral cortex tissue were quick-frozen in liquid nitrogen and stored at -80˚C for future use. Total RNAs were extracted with TRIzol reagent, quantified (NanoDrop ND-2000; Thermo Fisher Scientific, Inc., Pittsburgh, PA, USA), and analyzed for integrity (Agilent Bioanalyzer 2100; Agilent Technologies, Inc., Santa Clara, CA, USA). RNA labeling and microarray hybridization were performed according to standard protocols provided by the manufacturer.

LncRNA and mRNA microarray expression profiling. Total RNAs (100 ng) were labeled with the mRNA Complete Labeling and Hyb kit and hybridized on OE Biotech Rat lncRNA Microarray v2.0 8x60K (both Agilent Technologies, Inc.). This microarray contained 40,367 probes for 30,367 rat mRNAs and 10,000 rat lncRNAs derived from authoritative databases, including Ensembl, RefSeq, Ultra-conserved region encoding LncRNA (UCR), and lncRNAdb.

Reverse transcription-quantitative polymerase chain reaction (RT-qPCR). To validate the differentially expressed lncRNAs, quantitative RT-PCR was performed using a two-step reaction, which included RT and PCR, according to the manufacturer's instructions. Each RT reaction consisted of 0.5 μg of RNA, 2 μl of PrimerScript Buffer, 0.5 μl of oligo dT, 0.5 μl of random 6-mers, and 0.5 μl of PrimerScript RT Enzyme Mix I (Takara Bio, Inc., Otsu, Japan) in a total volume of 10 μl. RT reactions were performed in a GeneAmp® PCR System 9700 (Applied Biosystems; Thermo Fisher Scientific, Inc.) for 15 min at 37˚C followed by heat inactivation for 5 sec at 85˚C. The 10 μl RT reaction mix was then diluted 10-fold in nuclease-free water and stored at -20˚C. RT-qPCR was performed with 10 μl of a PCR reaction mixture that contained 1 μl of cDNA, 5 μl of 2X LightCycler® 480 SYBR-Green I Master Mix, 0.2 μl of forward primer, 0.2 μl of reverse primer, and 3.6 μl of nuclease-free water in a LightCycler® 480 II Real-time PCR Instrument (both Roche Applied Science, Rotkreuz, Switzerland). Reactions were incubated in a 384-well optical plate (Roche) at 95˚C for 10 min followed by 40 cycles of 95˚C for 10 sec and 60˚C for 30 sec. Each sample was run in triplicate and a melting curve analysis was performed at the end of each PCR cycle to specifically validate generation of the expected PCR product. The expression levels of lncRNAs were normalized to glyceraldehyde-3-phosphate dehydrogenase expression and were calculated using the $2^{-\Delta\Delta Cq}$ method. Primers were synthesized by Generay Biotech (Generay, Shanghai, China) based on mRNA sequences in the NCBI database and the sequences are given in Table I.

Analyses of microarray results and predictions of lncRNA functions. After differentially expressed mRNA and lncRNA data from microarrays were acquired, raw signals were $\log_2$ transformed. Differentially expressed mRNAs and lncRNAs were screened for absolute values of fold change (FC) >2 and P-values <0.05 (Student's t-test). The differentially expressed mRNAs were submitted to the DAVID database (http://david.abcc.ncifcrf.gov) and were classified into different annotation groups by Gene Ontology (GO) and Kyoto Encyclopedia of Genes and Genomes (KEGG) analyses. Distinguishable gene expression patterns were displayed by hierarchical clustering.

Statistical analysis. All statistical analyses were performed using the SPSS software 13.0 (SPSS, Inc., Chicago, IL, USA). Data were presented as mean ± SD or proportions as appropriate. Unpaired student t-test were performed to compare the differences of NDS, apoptotic cells, and validating lncRNA expressions between two groups, and correlations were calculated using Spearman's correlation coefficient, which is the

Table I. Primers for validation of differentially expressed long noncoding RNAs.

Gene symbol	Forward primer (5'-3')	Reverse primer (5'-3')
TCONS_00097275	GCCACCAGGACTGATAAT	TGTGTGTGTGTGTGTACG
TCONS_00077647	ATGGTGATTCGCACTTGT	TCCTTTAGCTCAGACTGGC
TCONS_00132873	GTTCAGGCAAGCTCCAAA	ATCCGTGTCTGGAACATT
TCONS_00066427	CAGGTCTTCTTTACCACCGA	GAGAGCAGGCAGAAGTGA
NR_002597.1	GCTGTGAGATGCAGGACAA	AAGGTGGCTGCTGTATATT
TCONS_00079198	GAAGGAGTGTGGAACTCAAC	CCTCTGCCATTAGACTTTGT
GAPDH	GCGAGATCCCGCTAACATCA	CTCGTGGTTCACACCCATCA

Pearson's correlation coefficient of the indexed ranks of the two data sets. P<0.05 by two-tailed t-test was considered to indicate a statistically significant difference.

Results

The severity of brain damage of rats after ROSC 24 h. The induction of VF caused serious injury to the brain in rats after ROSC 24 h in CPR group, 3 rats were dead within 24 h, and the other 6 rats were survival to 24 h. All rats in Sham group were alive to the end of the experiment. The NDS score in CPR group were 394±95, significantly higher than 0±0 in Sham group (P<0.001). The TUNEL staining showed that the induction of VF significantly increased the amount of apoptotic cells in the cortex, compared with that in Sham group (Fig. 1).

Changes in lncRNA and mRNA expressions in the CA and BC groups. From the lncRNA microarray, we found 58 lncRNA transcripts that were differentially expressed. Thirty-seven of the lncRNA transcripts were upregulated and 21 of the lncRNA transcripts were downregulated in the CA group when compared with the BC group (Table II). The TCONS_00045076 (probe CUST_12461 _PI429484123) and TCONS_00087195 (probe CUST_12461_PI429484123) lncRNAs were the most upregulated and downregulated transcripts in the CA group, respectively. According to absolute FC values (abs), the differentially expressed lncRNA transcripts were divided into two groups: five transcripts with FC values between 5 and 10 (highly dysregulated lncRNAs) and 53 transcripts with FC values between 2 and 5 (less dysregulated lncRNAs).

Using the same criteria that we used for the lncRNAs, we found 258 differentially expressed mRNA transcripts. 177 of the transcripts in the CA group were upregulated and 81 of the transcripts in the CA group were downregulated when compared with the BC group. The NM_001106299 (A_43_P16887) and NM_001033691 (A_44_P1039994) mRNAs were the most upregulated and downregulated transcripts in the CA group, respectively. Some of the differentially expressed mRNAs (FC>4) are listed in Table III; the un-named mRNAs are listed by their probe names, such as A_44_P809486.

The microarray data were uploaded to the GEO database (GEO no. GSE108342; https://www.ncbi.nlm.nih.gov/geo/query/acc.cgi?acc=GSE108342).

Validation of lncRNA microarray. To validate the lncRNA microarray results, three upregulated and two downregulated lncRNAs were randomly selected from the 58 differentially expressed lncRNAs and their expressions were analyzed in five CA tissues and in four BC tissues using RT-qPCR. The RT-qPCR results were consistent with the microarray results, and RT-qPCR

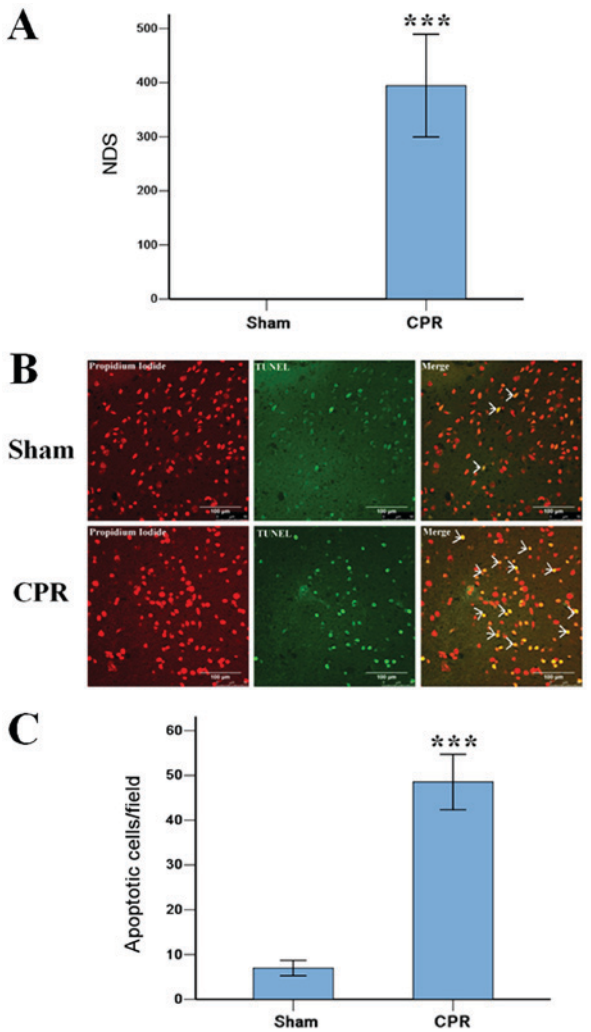

Figure 1. Severity of brain damage post cardiac arrest. (A) The NDS were 394±95 and 0±0 in the CPR and Sham groups, respectively. (B) TUNEL staining revealed that the induction of VF induced severe injury to the brain. TUNEL positive cells are yellow and are indicated by white arrows (scale bars, 50 μm). (C) The number of apoptotic cells in the cortex were significantly increased compared with the Sham group (48±6 vs. 7±2/field). Data are presented as the mean ± standard deviation. ***P<0.001 vs. Sham. NDS, neurological deficits scores; TUNEL, TdT-mediated dUTP-biotin nick end labeling; CPR, cardiopulmonary resuscitation; VF, ventricular fibrillation.

Table II. Differentially expressed long noncoding RNAs in cardiac arrest-return of spontaneous circulation.

No.	lncRNA	FC (abs)	Regulation	BC	CA	Chromosome no.
1	TCONS_00045076	8.07	Up	2.60±2.54	5.61±0.94	14
2	TCONS_00097275	8.00	Up	2.31±1.87	5.31±0.78	4
3	TCONS_00097694	6.75	Up	2.59±2.36	5.34±1.05	4
4	TCONS_00058731	6.27	Up	2.67±1.53	5.32±0.36	17
5	ENSRNOT00000031100	5.38	Up	4.59±1.48	7.02±0.59	15
6	TCONS_00045077	4.47	Up	4.13±1.60	6.29±0.94	Un_random
7	XR_146410.1	4.09	Up	4.78±1.13	6.81±0.96	Un
8	TCONS_00064719	4.06	Up	4.55±1.23	6.57±0.89	Un_random
9	XR_146719.1	3.70	Up	4.27±1.27	6.15±0.68	Un
10	ENSRNOT00000058957	3.69	Up	7.88±0.38	9.76±0.58	X
11	ENSRNOT00000030838	3.36	Up	8.37±0.22	10.12±0.53	3
12	XR_146012.1	3.34	Up	7.34±0.83	9.08±0.59	5
13	XR_146595.1	3.08	Up	3.62±0.76	5.24±0.47	14
14	TCONS_00040687	3.08	Up	4.27±0.71	5.90±0.59	13
15	XR_147150.1	3.03	Up	5.74±0.80	7.34±0.73	Un
16	XR_146408.1	2.85	Up	5.48±0.89	6.99±0.61	Un
17	TCONS_00062712	2.84	Up	3.29±1.11	4.80±0.27	18
18	TCONS_00113107	2.76	Up	4.69±0.55	6.16±0.45	6
19	TCONS_00122410	2.74	Up	3.52±0.40	4.98±0.99	7
20	TCONS_00046288	2.68	Up	3.01±0.26	4.44±0.58	15
21	TCONS_00009008	2.59	Up	3.97±0.60	5.34±0.61	1
22	TCONS_00008734	2.48	Up	3.22±0.99	4.53±0.48	1
23	TCONS_00066427	2.30	Up	9.68±0.75	10.88±0.59	2
24	TCONS_00041399	2.28	Up	2.92±0.60	4.11±0.53	14
25	ENSRNOT00000065794	2.25	Up	3.81±0.64	4.98±0.47	8
26	TCONS_00062192	2.24	Up	3.52±0.32	4.69±0.28	18
27	TCONS_00051727	2.20	Up	3.46±0.86	4.60±0.27	16
28	TCONS_00048046	2.20	Up	4.43±0.70	5.57±0.49	15
29	FR144720	2.16	Up	3.39±0.51	4.50±0.59	1
30	ENSRNOT00000074021	2.14	Up	5.38±0.50	6.48±0.61	2
31	TCONS_00132873	2.11	Up	8.84±0.69	9.91±0.63	12
32	TCONS_00065841	2.10	Up	3.61±0.79	4.68±0.47	19
33	TCONS_00054776	2.08	Up	4.69±0.39	5.75±0.35	16
34	TCONS_00054777	2.08	Up	3.50±0.77	4.56±0.24	16
35	uc.280+	2.07	Up	6.95±0.69	8.01±0.39	3
36	ENSRNOT00000040695	2.04	Up	6.57±0.09	7.60±0.32	X_random
37	uc.129+	2.02	Up	6.72±0.44	7.73±0.55	2
38	TCONS_00087195	3.74	Down	5.15±0.49	3.25±0.55	3
39	TCONS_00129724	3.49	Down	4.77±0.85	2.96±0.57	8
40	TCONS_00077647	3.27	Down	7.78±1.02	6.07±0.68	20
41	TCONS_00072164	3.16	Down	4.96±0.34	3.30±1.31	2
42	NR_002597.1	2.92	Down	8.97±1.07	7.42±0.48	20
43	TCONS_00079198	2.73	Down	6.78±0.85	5.33±0.59	20
44	TCONS_00046110	2.69	Down	6.54±0.62	5.11±0.99	15
45	TCONS_00016640	2.64	Down	5.00±0.28	3.60±0.45	1
46	TCONS_00106864	2.38	Down	5.60±0.27	4.35±0.81	5
47	TCONS_00098087	2.37	Down	4.94±0.43	3.69±0.08	4
48	TCONS_00138507	2.36	Down	5.87±0.45	4.63±0.95	X
49	NR_037614.1	2.35	Down	5.90±0.22	4.66±0.94	8
50	XR_145894.1	2.34	Down	5.56±0.72	4.34±0.38	3
51	TCONS_00132190	2.23	Down	7.32±0.84	6.17±0.58	9
52	TCONS_00040199	2.22	Down	5.07±0.58	3.92±0.68	13

Table II. Continued.

No.	lncRNA	FC (abs)	Regulation	BC	CA	Chromosome no.
53	TCONS_00040514	2.16	Down	4.91±0.52	3.80±0.76	13
54	XR_145922.1	2.14	Down	8.05±0.69	6.95±0.43	4
55	TCONS_00062765	2.10	Down	5.11±0.73	4.04±0.53	18
56	TCONS_00021035	2.05	Down	5.72±0.19	4.69±0.53	10
57	TCONS_00066438	2.04	Down	4.18±0.21	3.15±0.68	n/a
58	TCONS_00122316	2.00	Down	3.84±0.39	2.83±0.71	7

BC and CA data are presented as the mean ± standard deviation. FC (abs), absolute fold change; BC, blank control; CA, cardiac arrest; n/a, not available.

demonstrated that the TCONS_00079198 lncRNA transcript was differentially expressed ($P<0.05$ using the $2^{-\Delta\Delta Ct}$ method; Fig. 2). RT-qPCR analysis of the other lncRNAs transcripts demonstrated that the differential expressions were consistent with the microarray data, but were not significant ($P>0.05$).

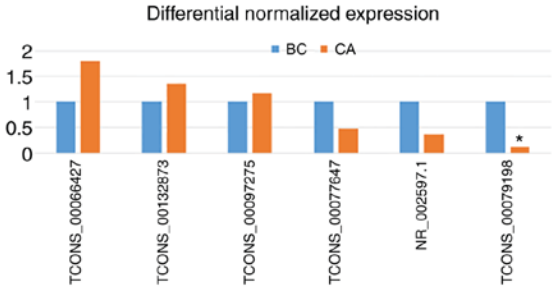

Figure 2. Validation of long noncoding RNA microarray. *P<0.05 vs. blank control (BC group).

Hierarchical clustering analysis. Differentially expressed lncRNA data were used to generate a heat map analysis of unsupervised hierarchical clustering. The differentially expressed lncRNAs clearly segregated into BC and CA clusters (Fig. 3) indicating that there was a significant difference in the lncRNA expression profiles between the CA and BC groups.

LncRNA and mRNA coexpression profiles. To compare lncRNA profiles with their corresponding mRNA network profiles, we calculated the Pearson correlation for the expression value of each lncRNA with the expression value of each mRNA for paired CA and BC samples (Fig. 4). Differentially expressed lncRNAs were coexpressed with thousands of mRNAs. For instance, TCONS_00087195 was coexpressed with 1,402 mRNA transcripts, and TCONS_00045076 was coexpressed with 1,293 mRNA transcripts. The top five mRNAs that correlated with TCONS_00087195 were Tcp1l1, Ppp1r15a, Asgr2, Htra4, and LOC691666, and the top five mRNAs that correlated with TCONS_00045076 were Lypd1, Fign, LOC100913068, Kcnv2, and Pcdh17. Of the 58 lncRNAs, 40 are predicted to regulate Btg1, 36 are predicted to regulate Acot12, 36 are predicted to regulate Fam65b, 41 are predicted to regulate Gm8430, 38 are predicted to regulate Hnrph1, 40 are predicted to regulate Pou6f1, 40 are predicted to regulate Sap30l, 36 are predicted to regulate Vrk1, and 38 are predicted to regulate Zfp454 (Fig. 4). These data indicate that differentially expressed lncRNAs potentially regulate mRNA expression and form a complex lncRNA-mRNA interaction network during CA.

Predictions of lncRNA functions during CA pathology. We found that each differentially expressed lncRNA associated with numerous differentially expressed mRNAs involved in multiple processes, and our data indicated that these lncRNA-mRNA networks play potentially important roles in pathological processes during CA. Thus, we made functional predictions based on GO and KEGG pathway annotations of differentially expressed lncRNAs and data on the corresponding coexpressed mRNAs. The differentially expressed lncRNAs could be grouped into numerous signaling pathways and processes (Figs. 5 and 6). The relationships between differentially expressed lncRNAs and their functional annotations were predicted by the top 200 and top 500 GO pathway annotations sorted by q-value, frequency counting, and statistical function annotation according to component, function, and pathway process, respectively. For example, in the top 200 GO pathway enrichments (Fig. 5A), the most frequent predictions were cytosol, voltage-gated potassium channel complex, neuron projection, cytoplasm, and nucleolus with regards to the pathways annotated by components. With regards to the pathways annotated by function, the most frequent predictions were sequence-specific DNA binding, dopachrome isomerase activity, protein serine/threonine kinase activity, N-terminal myristoylation domain binding, protein phosphatase activator activity, and transcription regulatory region DNA binding. With regards to the pathways annotated by process, the most frequent predictions were positive regulation of apoptotic process, membrane depolarization, potassium ion transmembrane transport, apoptotic process, homophilic cell adhesion, substrate-dependent cell migration, growth plate cartilage development, and response to cold. In the top 500 GO pathway enrichments, (Fig. 5B), the most frequent component predictions were dendrite, cytosol, voltage-gated potassium channel complex, cytoplasm, nucleus, nucleolus, synapse, neuronal cell body, hemoglobin complex, neuron projection, perinuclear region of cytoplasm, AIM2 inflammasome complex, NLRP3 inflammasome complex, and perikaryon. The most frequent function predictions were sequence-specific DNA binding,

Table III. Differentially expressed mRNAs in cardiac arrest-return of spontaneous circulation.

No.	mRNA	FC (abs)	Regulation	BC	CA	Chromosome no.
1	Ahsp	38.62	Up	1.98±3.43	7.25±2.12	1
2	Ptges	18.56	Up	3.27±3.51	7.48±0.88	3
3	Egr4	13.98	Up	2.45±2.89	6.25±1.23	4
4	Six3	11.17	Up	2.93±3.11	6.41±0.95	6
5	Apold1	10.84	Up	4.44±2.56	7.87±0.94	4
6	Gch1	10.10	Up	3.21±2.34	6.55±1.17	15
7	Msantd1	9.23	Up	2.40±2.07	5.60±0.75	14
8	A_64_P010891	7.52	Up	2.83±1.98	5.74±1.51	17
9	Trh	7.39	Up	2.30±1.37	5.19±0.71	4
10	Nr4a1	6.64	Up	8.15±1.55	10.88±0.58	7
11	Gdf15	5.72	Up	3.55±1.63	6.06±0.44	16
12	Ptgs2	5.33	Up	5.71±1.31	8.13±0.93	13
13	LOC688972	5.31	Up	3.60±0.45	6.01±1.69	19
14	A_64_P058988	4.83	Up	3.79±0.86	6.07±1.28	19
15	Grin3b	4.72	Up	3.47±1.69	5.71±0.65	7
16	A_44_P386579	4.69	Up	3.68±1.83	5.90±0.66	18
17	Gadd45g	4.66	Up	7.14±1.76	9.36±0.60	17
18	A_64_P065301	4.65	Up	4.64±1.82	6.86±0.89	Un
19	A_64_P134263	4.63	Up	3.99±1.67	6.20±0.79	Un
20	Tacr1	4.44	Up	2.80±1.62	4.95±0.51	4
21	Kcnv2	4.43	Up	4.63±1.57	6.78±0.35	1
22	Cenpf	4.40	Up	2.55±1.61	4.68±0.99	13
23	Mt1a	4.29	Up	9.24±0.57	11.34±0.55	19
24	LOC287167	4.29	Up	5.25±1.57	7.35±0.86	10
25	Tmem252	4.26	Up	5.34±1.72	7.43±0.26	1
26	LOC100362110	4.17	Up	5.25±1.39	7.31±0.25	13
27	LOC685488	4.12	Up	4.87±1.36	6.91±0.79	19
28	Nr4a2	4.07	Up	7.36±0.95	9.39±1.07	3
29	Irf7	12.31	Down	8.27±1.66	4.65±2.63	1
30	RT1-A2	9.38	Down	10.74±1.30	7.51±2.07	20
31	RT1-M6-1	7.73	Down	5.98±0.29	3.03±2.30	20
32	A_44_P884971	6.99	Down	5.53±0.39	2.72±2.23	9
33	Olr59	6.30	Down	5.11±0.49	2.46±2.07	1
34	A_64_P033885	5.90	Down	5.63±1.04	3.07±1.92	18
35	Enthd1	5.80	Down	4.83±0.71	2.30±1.98	7
36	L2hgdh	5.20	Down	6.05±0.50	3.67±1.22	6
37	Osr1	4.95	Down	7.59±0.36	5.28±1.68	6
38	Lrrc17	4.93	Down	5.20±0.79	2.90±1.67	4
39	Tnfsf10	4.83	Down	6.66±1.00	4.39±0.69	2
40	Adam33	4.46	Down	5.04±0.37	2.88±1.00	3
41	Ltbp2	4.19	Down	5.32±0.87	3.25±0.74	6
42	RGD1563091	4.03	Down	5.68±0.80	3.66±0.93	4

FC, fold change; BC, blank control; CA, cardiac arrest.

dopachrome isomerase activity, protein serine/threonine kinase activity, protein phosphatase activator activity, and voltage-gated potassium channel activity. The most frequent process predictions were potassium ion transmembrane transport, regulation of ion transmembrane transport, response to light stimulus, membrane depolarization, positive regulation of apoptotic process, homophilic cell adhesion, regulation of cell proliferation, protein autophosphorylation, apoptotic process, positive regulation of ryanodine-sensitive calcium-release channel activity, aging, response to mechanical stimulus, substrate-dependent cell migration, transcription, DNA-templated, and response to cold.

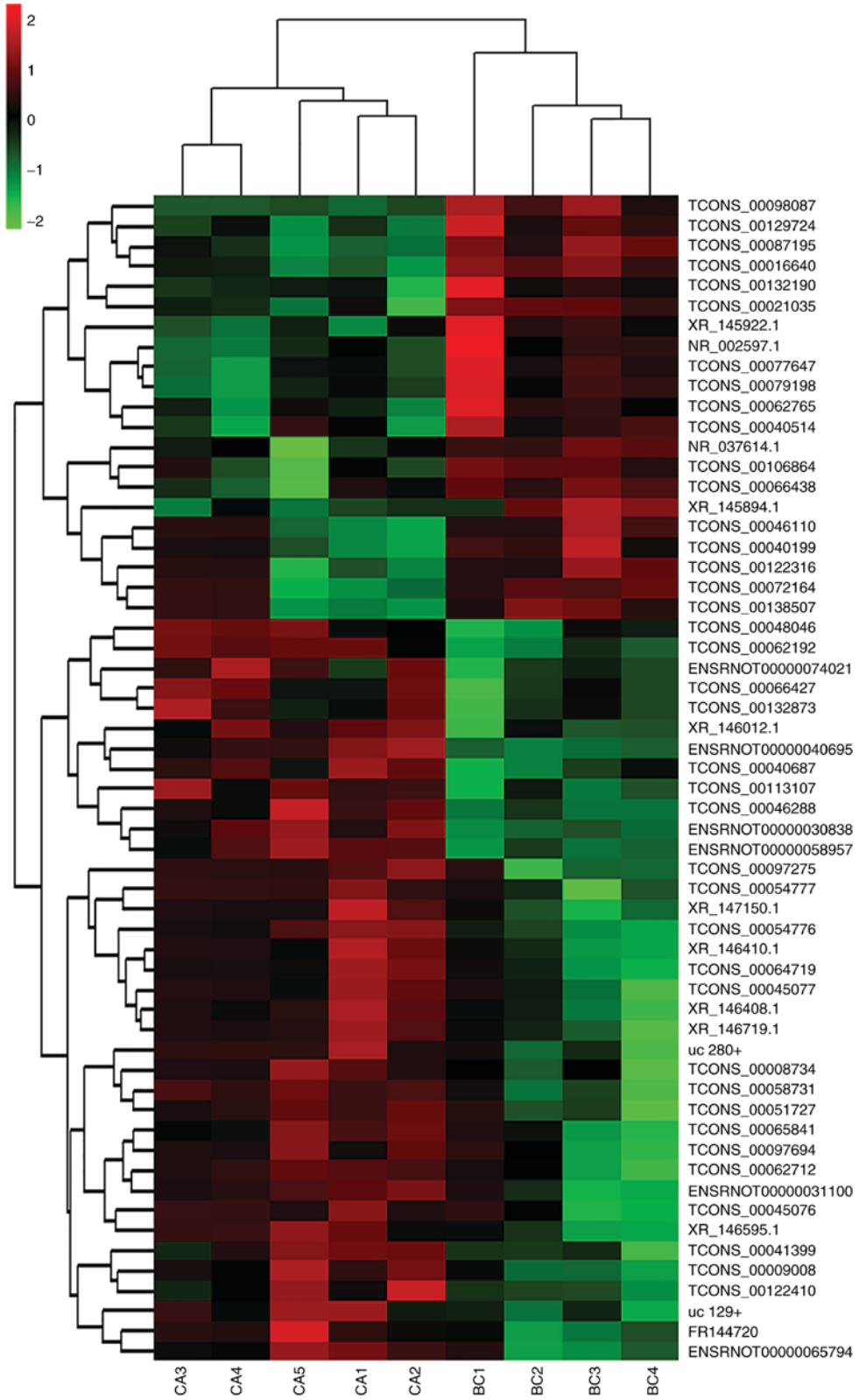

Figure 3. Heat map comparing differentially expressed lncRNAs in BC brain samples and in CA brain samples. The differentially expressed lncRNAs segregated into BC and CA clusters. Each row represents one lncRNA, and each column represents one tissue sample. The relative lncRNA expression is depicted according to the color scale. Red and green indicates upregulation and downregulation, respectively. The values of 2.0, 0 and -2.0 are the fold changes depicted in the color spectrum. lncRNA, long noncoding RNA; BC, blank control; CA, cardiac arrest.

KEGG pathway annotations of differentially expressed lncRNAs and their corresponding coexpressed mRNAs were performed to predict lncRNA functions during CA pathology (Fig. 6). In the top 200 KEGG pathway enrichments (Fig. 6A), the most frequent predictions were the MAPK signaling pathway, amphetamine addiction, adrenergic signaling in cardiomyocytes, the GnRH signaling pathway, insulin secretion, dopaminergic synapse, glutamatergic synapse, the

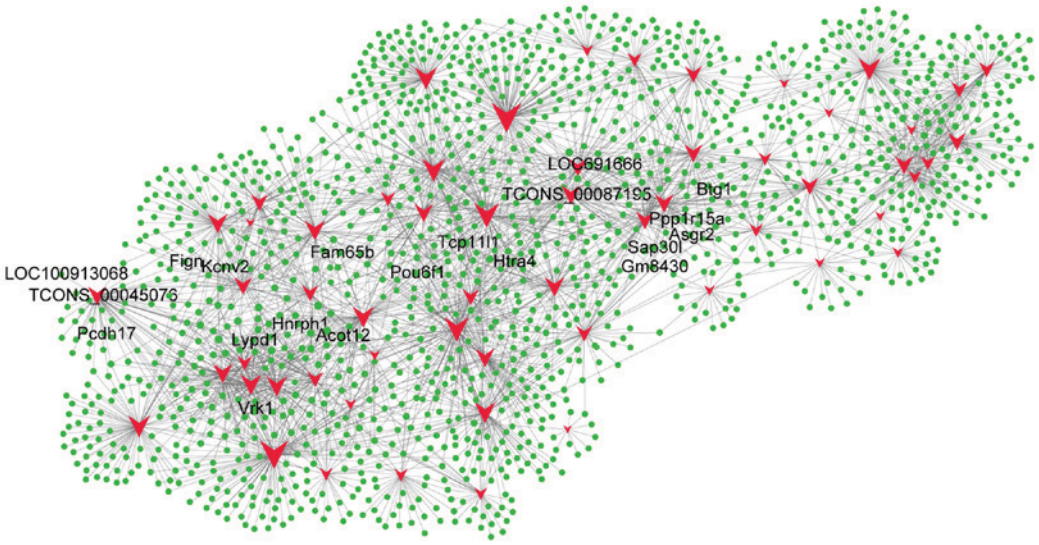

Figure 4. The majority of the mRNAs were predicted to be regulated by the differentially expressed lncRNAs. The top lncRNA-mRNA pairs are the most credible. Solid green circles represent mRNAs and solid red arrowheads represent lncRNAs. The edges between the circles and the arrowheads indicate potential regulation of the mRNAs by the lncRNAs. lncRNA, long noncoding RNA; mRNA, messenger RNA.

cAMP signaling pathway, the estrogen signaling pathway, antigen processing and presentation, gastric acid secretion, the TNF signaling pathway, gap junction, and the calcium signaling pathway. In the top 500 KEGG pathway enrichments (Fig. 6B), the most frequent predictions were the MAPK signaling pathway, amphetamine addiction, adrenergic signaling in cardiomyocytes, the GnRH signaling pathway, insulin secretion, gap junction, dopaminergic synapse, the oxytocin signaling pathway, and the glutamatergic synapse. In summary, the most common KEGG pathways and GO pathways involved in CA were signaling pathways, apoptotic processes, inflammation, and synaptic processes. For example, in the KEGG enrichment, for the most downregulated lncRNA TCONS_00087195, the most frequently predicted functions involved the Ras signaling pathway, amphetamine addiction, and dopaminergic synapse. For the second-most downregulated lncRNA TCONS_00129724, the most frequently predicted functions involved the TNF signaling pathway, the NF-κ B signaling pathway, and the Jak-STAT signaling pathway. For the third-most downregulated lncRNA TCONS_00077647, the most frequently predicted functions involved the RIG-I-like receptor signaling pathway, the MAPK signaling pathway, and cytosolic DNA sensing. However, for the most upregulated lncRNA TCONS_00045076, the most frequently predicted function was protein processing in the dopaminergic and glutamatergic synapse. For the second-most upregulated lncRNA TCONS_00097275, the most frequently predicted functions involved protein processing in the dopaminergic synapse, the estrogen signaling pathway, and TNF signaling. For the third-most upregulated lncRNA TCONS_00097694, the most predicted functions involved the glutamatergic synapse, the dopaminergic synapse, and cAMP signaling. As expected, one lncRNA can participate in multiple KEGG pathways and both upregulated and downregulated lncRNAs could be involved in some of the same processes, such as the TNF signaling pathway and the dopaminergic synapse, indicating that lncRNAs play complex roles in CA pathology.

Discussion

In the present study, we investigated lncRNA and mRNA profiles in a CA-ROSC rat model during an early stage of reperfusion using high-throughput lncRNA and mRNA microarrays. The lncRNA microarray showed that 58 lncRNAs were differentially expressed in the CA brain; 37 of the lncRNAs were upregulated and 21 of the lncRNAs were downregulated when compared with the control samples. The mRNA microarray showed that 258 mRNA transcripts were differentially expressed in the CA brain; 177 of the mRNAs were upregulated and 81 of the mRNAs were downregulated. We investigated the relationships between these lncRNAs and mRNAs and found that each differentially expressed lncRNA was coexpressed with thousands of mRNAs. Furthermore, we predicted the functions of these differentially expressed lncRNAs with their corresponding coexpressed mRNAs and found that hundreds of pathway annotations were enriched in both GO and KEGG analyses. The predicted functions of lncRNAs were primarily related to protein voltage-gated potassium channel complexes, serine/threonine kinase activity, protein phosphatase activator activity, the MAPK signaling pathway, and apoptotic processes.

Previous studies have shown that ischemia leads to extensive changes in cerebral lncRNA expression in rodents (12,16), but the cerebral lncRNA expression profile and the potential roles of lncRNAs during the early stages of reperfusion remain unknown. The present study is the first that synchronously examined genome-wide lncRNA and mRNA expression patterns and their network profiles in a CA-ROSC model and that discovered extensive alterations in expression of lncRNAs and their corresponding mRNAs as a result of CA-ROSC.

In the present study, we found that CA-ROSC markedly altered expression of mRNAs involved in vital metabolic pathways, such as inflammatory and apoptotic pathways. In addition, we found that lncRNAs coregulate expression of the differentially expressed mRNAs. Some of the differentially mRNAs identified in our study have also been identified in other

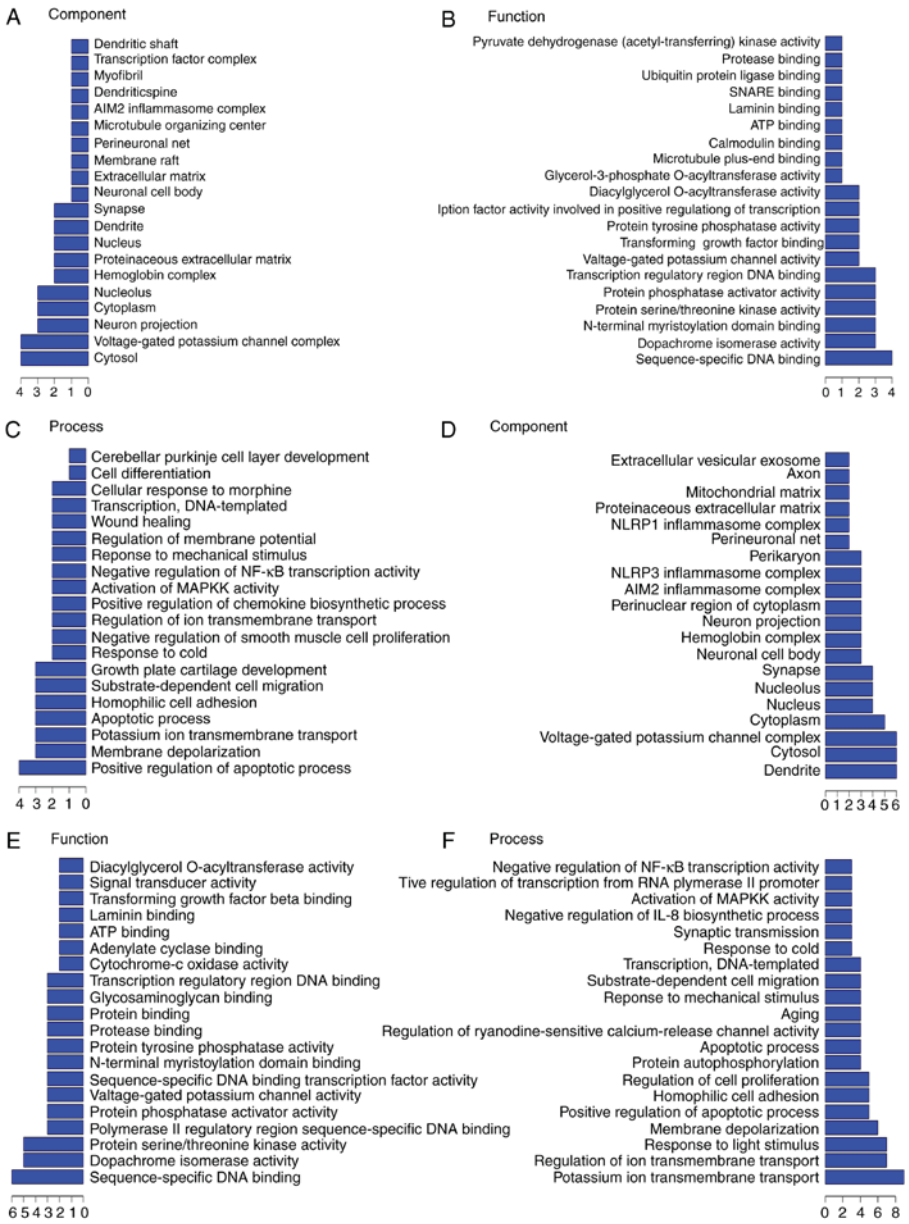

Figure 5. GO analysis. (A-C) The top 200 pathways enriched in GO and (D-F) the top 500 pathways enriched in GO. GO, gene ontology.

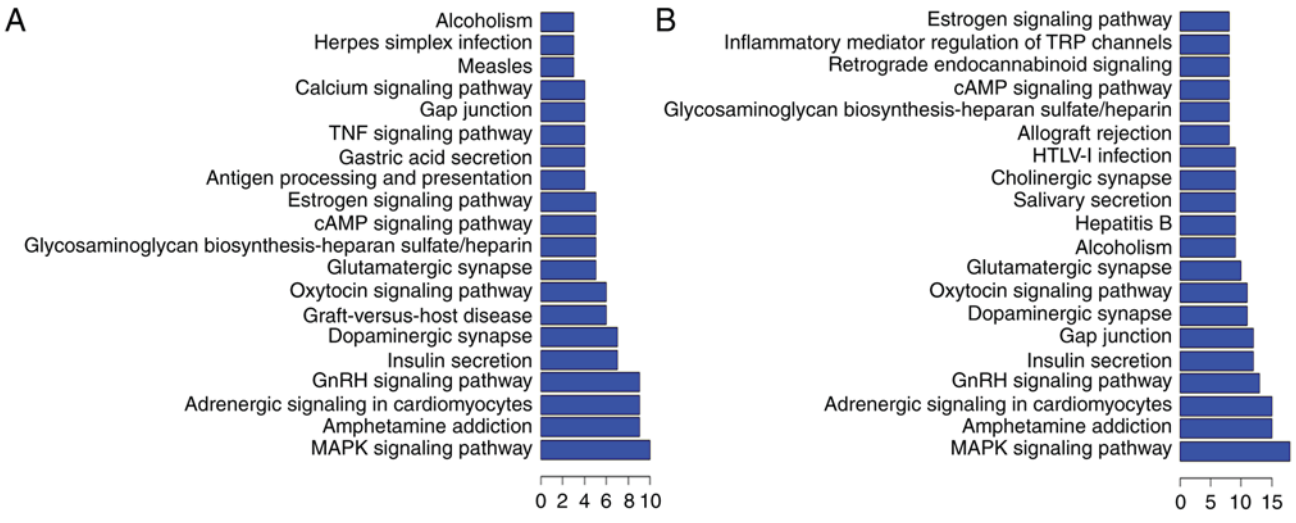

Figure 6. KEGG analysis. (A) The top 200 pathways enriched in KEGG and (B) the top 500 pathways enriched in KEGG. KEGG, Kyoto Encyclopedia of Genes and Genomes.

Table IV. A brief summary of the literature on differentially expressed mRNAs in cardiac arrest-return of spontaneous circulation and ischemia.

Author, year	mRNA	Animal	Literature title	(Refs.)
Norman *et al*, 2011	Tumor necrosis factor	Adult male C57BL/6 mice	Cardiopulmonary arrest and resuscitation disrupts cholinergic anti-inflammatory processes: A role for cholinergic α7 nicotinic receptors.	(35)
Hu *et al*, 2013		Male Wistar rats (15-16 months)	Ulinastatin attenuates oxidation, inflammation and neural apoptosis in the cerebral cortex of adult rats with ventricular fibrillation after cardiopulmonary resuscitation.	(36)
Kaneko and Kibayashi, 2012		ddY mice and Swiss-Webster mice	Mild hypothermia facilitates the expression of cold-inducible RNA-binding protein and heat shock protein 70.1 in mouse brain.	(37)
Anju *et al*, 2011	Glutamate decarboxylase mRNA	Wistar neonatal rats (4-days)	Decreased GABAB receptor function in the cerebellum and brain stem of hypoxic neonatal rats: Role of glucose, oxygen and epinephrine resuscitation.	(38)
Tyree *et al*, 2006	Early Growth Response mRNA	Newborn piglets	Impact of room air resuscitation on early growth response gene-1 in a neonatal piglet model of cerebral hypoxic ischemia.	(39)
Vincze *et al*, 2010	Transforming growth factors-β1, -2 and -3	Rat	Distribution of mRNAs encoding transforming growth factors-β1, -2, and -3 in the intact rat brain and after experimentally induced focal ischemia.	(40)
Zhu *et al*, 2001	Transforming growth factor-β1	Rat	β2-adrenoceptor stimulation enhances latent transforming growth factor-β-binding protein-1 and transforming growth factor-β1 expression in rat hippocampus after transient forebrain ischemia.	(41)

ischemia studies (Table IV). To gain insight into the potential roles of the differentially expressed lncRNAs and mRNAs, we performed GO and KEGG pathway analyses to predict their biological functions during CA-ROSC. We found that the differentially expressed lncRNAs may be involved in protein voltage-gated potassium channel complexes, serine/threonine kinase activity, protein phosphatase activator activity, the MAPK signaling pathway, and apoptotic processes. These proteins and kinases are key enzymes in metabolic, inflammatory, and apoptotic pathways, which have been shown to be involved in I/R injuries (17-20). These results indicated that lncRNAs in the cerebral region may participate in pathological processes after CA-ROSC by promoting post-ischemic pathologies, including ionic imbalance, receptor dysfunction, and the inflammatory response during the early stages of reperfusion.

For the downregulated lncRNAs, the most frequent predicted functions enriched in the KEGG analysis involved the Ras signaling pathway, amphetamine addiction, the NF-κ B signaling pathway, the Jak-STAT signaling pathway, the RIG-I-like receptor signaling pathway, the MAPK signaling pathway, and the cytosolic DNA sensing pathway. Previous studies have shown that some of these pathways, such as the Ras signaling pathway (21), the NF-κ B signaling pathway (22,23), the Jak-STAT signaling pathway (24), the RIG-I-like receptor signaling pathway (25), the cytosolic DNA sensing pathway (25), and the MAPK signaling pathway (26,27) are involved in CA-ROSC and I/R injury. In addition, the cocaine- and amphetamine-regulated transcript (CART), which codes for a neuropeptide involved in amphetamine addiction has also been shown to play a neuroprotective role in cerebral ischemia and reperfusion (I/R) injury (28,29).

The most frequent predicted functions of the upregulated lncRNAs involve protein processing during glutamatergic synapsis (30), the estrogen signaling pathway (26), and the cAMP signaling pathway (31,32), which play vital roles in cerebral ischemia and reperfusion injury. In summary, our data indicated that the lncRNA-mRNA network interactions have potentially complex roles in cerebral I/R injury. Both upregulated and downregulated lncRNAs were predicted to participate in pathological processes during cerebral I/R injury, such as dopaminergic synapsis and the TNF signaling pathway (33,34), indicating that lncRNAs work synergistically during I/R injury.

There were several limitations in our study. First, we only investigated differentially expressed lncRNAs and mRNAs in cerebral cortex tissue. Second, the time for CA sample collection lasted only eight min. However, the aberrant expressions of lncRNAs and mRNAs after CA-ROSC may have spatial and temporal patterns that we did not evaluate in this study. The samples used in this study were limited (five samples in the CA group and four samples in the BC group). More samples and future studies are required to verify these results.

In this study, we found that CA-ROSC led to extensive alterations in lncRNA and mRNA expression patterns, and these alterations may affect the mRNA transcription and protein translation of vital pathways during I/R injury. Thus, lncRNAs may be promising novel targets for the development of therapeutics to reduce cerebral damage. Future studies should determine whether modulating specific lncRNAs can prevent post-CA pathophysiological events and/or promote plasticity and regeneration.

Acknowledgements

Not applicable.

Funding

The present study was supported by funding from The National Nature Science Foundation of China (grant nos. 81272021 and 81571867), The Science and Technology Foundation of Guangdong Province, China (grant nos. 2012B061700046 and 2012B031800286), and The Research Program for Colleges and Universities in Guangzhou (grant no. 2012C054).

Availability of data and materials

The datasets used and/or analyzed during the current study are available in the Genome Expression Omnibus (GEO) repository, www.ncbi.nlm.nih.gov/geo/query/acc.cgi?acc=GSE108342.

Authors' contributions

CH and ZL conceived the idea for the study. CH, RL, MY, XZ and XLi contributed to the design, and performed the animal experiments and harvested samples. XLia and HW contributed to sample measurement procedures. ZZ and QL performed data analysis. CH, MY and RL wrote the manuscript, and CH and XZ revised the manuscript.

Ethics approval and consent to participate

The animal studies were approved by the Institutional Animal Care and Use Committee of Sun Yat-sen University (Guangdong, China) and the procedures used were in accordance with the Animal Research Reporting for *In Vivo* Experiments guidelines on animal research.

Consent for publication

Not applicable.

Competing interests

The authors declare that they have no competing interests.

References

1. Writing Group Members, Mozaffarian D, Benjamin EJ, Go AS, Arnett DK, Blaha MJ, Cushman M, Das SR, de Ferranti S, Després JP, *et al*: Executive summary: Heart disease and stroke statistics-2016 update: A report from the american heart association. Circulation 133: 447-454, 2016.
2. Neumar RW, Nolan JP, Adrie C, Aibiki M, Berg RA, Böttiger BW, Callaway C, Clark RS, Geocadin RG, Jauch EC, *et al*: Post-cardiac arrest syndrome: Epidemiology, pathophysiology, treatment, and prognostication. A consensus statement from the International Liaison Committee on Resuscitation (American Heart Association, Australian and New Zealand Council on Resuscitation, European Resuscitation Council, Heart and Stroke Foundation of Canada, InterAmerican heart foundation, Resuscitation Council of Asia, and the Resuscitation Council of Southern Africa); the American Heart Association Emergency Cardiovascular Care Committee; the Council on Cardiovascular Surgery and Anesthesia; the Council on Cardiopulmonary, Perioperative, and Critical care; the Council on Clinical Cardiology; and the Stroke Council. Circulation 118: 2452-2483, 2008.

3. Wang KC and Chang HY: Molecular mechanisms of long noncoding RNAs. Mol Cell 43: 904-914, 2011.
4. Khalil AM, Guttman M, Huarte M, Garber M, Raj A, Rivea Morales D, Thomas K, Presser A, Bernstein BE, van Oudenaarden A, *et al*: Many human large intergenic noncoding RNAs associate with chromatin-modifying complexes and affect gene expression. Proc Natl Acad Sci USA 106: 11667-11672, 2009.
5. Cabili MN, Trapnell C, Goff L, Koziol M, Tazon-Vega B, Regev A and Rinn JL: Integrative annotation of human large intergenic noncoding RNAs reveals global properties and specific subclasses. Genes Dev 25: 1915-1927, 2011.
6. Leung A, Trac C, Jin W, Lanting L, Akbany A, Sætrom P, Schones DE and Natarajan R: Novel long noncoding RNAs are regulated by angiotensin II in vascular smooth muscle cells. Circ Res 113: 266-278, 2013.
7. Bonasio R and Shiekhattar R: Regulation of transcription by long noncoding RNAs. Annu Rev Genet 48: 433-455, 2014.
8. Dong X, Yu LG, Sun R, Cheng YN, Cao H, Yang KM, Dong YN, Wu Y and Guo XL: Inhibition of PTEN expression and activity by angiotensin II induces proliferation and migration of vascular smooth muscle cells. J Cell Biochem 114: 174-182, 2013.
9. Qureshi IA and Mehler MF: Long non-coding RNAs: Novel targets for nervous system disease diagnosis and therapy. Neurotherapeutics 10: 632-646, 2013.
10. Yin KJ, Hamblin M and Chen YE: Non-coding RNAs in cerebral endothelial pathophysiology: Emerging roles in stroke. Neurochem Int 77: 9-16, 2014.
11. Antoniou D, Stergiopoulos A and Politis PK: Recent advances in the involvement of long non-coding RNAs in neural stem cell biology and brain pathophysiology. Front Physiol 5: 155, 2014.
12. Dharap A, Pokrzywa C and Vemuganti R: Increased binding of stroke-induced long non-coding RNAs to the transcriptional corepressors Sin3A and coREST. ASN Neuro 5: 283-289, 2013.
13. Kilkenny C, Browne WJ, Cuthill IC, Emerson M and Altman DG: Improving bioscience research reporting: The ARRIVE guidelines for reporting animal research. Osteoarthritis Cartilage 20: 256-260, 2012.
14. Lin JY, Liao XX, Li H, Wei HY, Liu R, Hu CL, Huang GQ, Dai G and Li X: Model of cardiac arrest in rats by transcutaneous electrical epicardium stimulation. Resuscitation 81: 1197-1204, 2010.
15. Chun-Lin H, Jie W, Xiao-Xing L, Xing L, Yu-Jie L, Hong Z, Xiao-Li J and Gui-Fu W: Effects of therapeutic hypothermia on coagulopathy and microcirculation after cardiopulmonary resuscitation in rabbits. Am J Emerg Med 29: 1103-1110, 2011.
16. Dharap A, Nakka VP and Vemuganti R: Effect of focal ischemia on long noncoding RNAs. Stroke 43: 2800-2802, 2012.
17. Xiang Y, Zhao H, Wang J, Zhang L, Liu A and Chen Y: Inflammatory mechanisms involved in brain injury following cardiac arrest and cardiopulmonary resuscitation. Biomed Rep 5: 11-17, 2016.
18. Uchino H, Ogihara Y, Fukui H, Chijiiwa M, Sekine S, Hara N and Elmér E: Brain injury following cardiac arrest: Pathophysiology for neurocritical care. J Intensive Care 4: 31, 2016.
19. Quillinan N, Herson PS and Traystman RJ: Neuropathophysiology of brain injury. Anesthesiol Clin 34: 453-464, 2016.
20. Quillinan N, Grewal H, Deng G, Shimizu K, Yonchek JC, Strnad F, Traystman RJ and Herson PS: Region-specific role for GluN2B-containing NMDA receptors in injury to Purkinje cells and CA1 neurons following global cerebral ischemia. Neuroscience 284: 555-565, 2015.
21. Yao C, Zhang J, Chen F and Lin Y: Neuroprotectin D1 attenuates brain damage induced by transient middle cerebral artery occlusion in rats through TRPC6/CREB pathways. Mol Med Rep 8: 543-550, 2013.
22. Wei X, Zhang B, Zhang Y, Li H, Cheng L, Zhao X, Yin J and Wang G: Hydrogen sulfide inhalation improves neurological outcome via NF-κB-mediated inflammatory pathway in a rat model of cardiac arrest and resuscitation. Cell Physiol Biochem 36: 1527-1538, 2015.
23. Tang ZX, Chen GX, Liang MY, Rong J, Yao JP, Yang X and Wu ZK: Selective antegrade cerebral perfusion attenuating the TLR4/NF-κB pathway during deep hypothermia circulatory arrest in a pig model. Cardiology 128: 243-250, 2014.
24. Ottani A, Neri L, Canalini F, Calevro A, Rossi R, Cappelli G, Ballestri M, Giuliani D and Guarini S: Protective effects of the melanocortin analog NDP-α-MSH in rats undergoing cardiac arrest. Eur J Pharmacol 745: 108-116, 2014.
25. Wang H, Wang G, Zhang L, Zhang J, Zhang J, Wang Q and Billiar TR: ADAR1 suppresses the activation of cytosolic RNA-sensing signaling pathways to protect the liver from ischemia/reperfusion injury. Sci Rep 6: 20248, 2016.
26. Lebesgue D, Chevaleyre V, Zukin RS and Etgen AM: Estradiol rescues neurons from global ischemia-induced cell death: Multiple cellular pathways of neuroprotection. Steroids 74: 555-561, 2009.
27. Jover-Mengual T, Zukin RS and Etgen AM: MAPK signaling is critical to estradiol protection of CA1 neurons in global ischemia. Endocrinology 148: 1131-1143, 2007.
28. Wang Y, Qiu B, Liu J, Zhu WG and Zhu S: Cocaine- and amphetamine-regulated transcript facilitates the neurite outgrowth in cortical neurons after oxygen and glucose deprivation through PTN-dependent pathway. Neuroscience 277: 103-110, 2014.
29. Bin J, Wang Q, Zhuo YY, Xu JP and Zhang HT: Piperphentonamine (PPTA) attenuated cerebral ischemia-induced memory deficits via neuroprotection associated with anti-apoptotic activity. Metab Brain Dis 27: 495-505, 2012.
30. Tjepkema-Cloostermans MC, Hindriks R, Hofmeijer J and van Putten MJ: Generalized periodic discharges after acute cerebral ischemia: Reflection of selective synaptic failure? Clin Neurophysiol 125: 255-262, 2014.
31. Steinberg SF, Alcott S, Pak E, Hu D, Protas L, Möise NS, Robinson RB and Rosen MR: beta(1)-Receptors increase cAMP and induce abnormal Ca(i) cycling in the German shepherd sudden death model. Am J Physiol Heart Circ Physiol 282: H1181-H1188, 2002.
32. Li P, Gu T, Wang C, Zhang G and Shi E: Neuregulin 1 attenuates neuronal apoptosis induced by deep hypothermic circulatory arrest through ErbB4 signaling in rats. J Cardiovasc Pharmacol 66: 551-557, 2015.
33. Wang W, Zhao L, Bai F, Zhang T, Dong H and Liu L: The protective effect of dopamine against OGD/R injury-induced cell death in HT22 mouse hippocampal cells. Environ Toxicol Pharmacol 42: 176-182, 2016.
34. Sui B, Li Y and Ma L: Postconditioning improvement effects of ulinastatin on brain injury following cardiopulmonary resuscitation. Exp Ther Med 8: 1301-1307, 2014.
35. Norman GJ, Morris JS, Karelina K, Weil ZM, Zhang N, Al-Abed Y, Brothers HM, Wenk GL, Pavlov VA, Tracey KJ and Devries AC: Cardiopulmonary arrest and resuscitation disrupts cholinergic anti-inflammatory processes: A role for cholinergic α7 nicotinic receptors. J Neurosci 31: 3446-3452, 2011.
36. Hu CL, Xia JM, Cai J, Li X, Liao XX, Li H, Zhan H, Dai G and Jing XL: Ulinastatin attenuates oxidation, inflammation and neural apoptosis in the cerebral cortex of adult rats with ventricular fibrillation after cardiopulmonary resuscitation. Clinics (Sao Paulo) 68: 1231-1238, 2013.
37. Kaneko T and Kibayashi K: Mild hypothermia facilitates the expression of cold-inducible RNA-binding protein and heat shock protein 70.1 in mouse brain. Brain Res 1466: 128-136, 2012.
38. Anju TR, Jayanarayanan S and Paulose CS: Decreased GABAB receptor function in the cerebellum and brain stem of hypoxic neonatal rats: Role of glucose, oxygen and epinephrine resuscitation. J Biomed Sci 18: 31, 2011.
39. Tyree MM, Dalgard C and O'Neill JT: Impact of room air resuscitation on early growth response gene-1 in a neonatal piglet model of cerebral hypoxic ischemia. Pediatric Res 59: 423-427, 2006.
40. Vincze C, Pál G, Wappler EA, Szabó ER, Nagy ZG, Lovas G and Dobolyi A: Distribution of mRNAs encoding transforming growth factors-beta1, -2, and -3 in the intact rat brain and after experimentally induced focal ischemia. J Comp Neurol 518: 3752-3770, 2010.
41. Zhu Y, Culmsee C, Roth-Eichhorn S and Krieglstein J: Beta(2)-adrenoceptor stimulation enhances latent transforming growth factor-beta-binding protein-1 and transforming growth factor-beta1 expression in rat hippocampus after transient forebrain ischemia. Neuroscience 107: 593-602, 2001.